

## 70.3: Current-Scaling a-Si:H TFT Pixel Electrode Circuit for AM-OLEDs

Hojin Lee and Jerzy Kanicki

Organic and Molecular Electronics Lab., Dept. of Electrical Engineering & Computer Science  
University of Michigan, Ann Arbor 48109, USA

Y. C. Lin and Han-Ping Shieh

Display Institute, National Chiao Tung University, Hsinchu 300, Taiwan

### Abstract

We fabricated and characterized the amorphous silicon thin-film transistor (a-Si:H TFT) pixel electrode circuit with current-scaling function that can be used for active-matrix organic light-emitting displays (AM-OLEDs). As expected from previously reported simulation results, fabricated circuit showed an acceptable current-scaling performance for a high-resolution AM-OLED based on a-Si:H TFTs.

### 1. Introduction

Over last several years, it was shown by several authors [1-5] that the current driving pixel electrode circuits are among the most desirable solutions for active-matrix organic light-emitting displays (AM-OLEDs). However, as display size and resolution increase, a large timing delay can be observed at a low data current and its importance increases with the display size [6]. To address this issue, several solutions have been proposed based on poly crystalline silicon thin-film transistor (TFT) technology such as current-mirror circuit [7, 8] and series-connected TFT circuit [9]. Besides poly-Si TFTs, we also proposed amorphous silicon TFT (a-Si:H TFT) based current-scaling pixel electrode circuit to address this problem [6, 10]. In this paper, for the first time, we report on the electrical characteristics of the fabricated pixel electrode circuit based on this design, and present its current-scaling function in comparison with the previously published results.

### 2. Fabrication of Pixel Electrode Circuit

First, chrome layer (Cr, 2000Å) was deposited on glass substrate by a sputtering method, then was patterned by photo-lithography process using wet-etching CR-7 solution (Mask #1) to define gate electrodes. After soaking in GP:H<sub>2</sub>O (1:15), acetone, and methanol, the substrate was rinsed in DI water for 10 minutes, and finally blown dry with the N<sub>2</sub> gas. Tri-layer composed of hydrogenated amorphous silicon nitride (a-SiN<sub>x</sub>:H, 3000Å) / intrinsic hydrogenated amorphous silicon (a-Si:H, 1500Å) / P-doped a-Si:H layer (n<sup>+</sup> a-Si:H, 200Å) was deposited next in multi-chamber plasma-enhanced chemical-vapor deposition (PECVD) system at 300°C. A gas mixture of SiH<sub>4</sub> and NH<sub>3</sub>, and SiH<sub>4</sub> and H<sub>2</sub> was used for a-SiN<sub>x</sub>:H and a-Si:H layer deposition, respectively. First n<sup>+</sup> a-Si:H layer was used to achieve a good ohmic contact to a-Si:H. After definition of the device active island by wet-etching (Mask #2), substrate was dipped in HF solution to remove native oxide before deposition of a second n<sup>+</sup> a-Si:H layer (300Å), which was used to realized an ohmic contact to edges of a-Si:H island. Next, molybdenum / aluminum / molybdenum (Mo/Al/Mo, 1000Å/3000Å/1000Å) multi-layer was deposited by thermal coater, and metal source / drain (S/D) contacts were defined by wet-etching (Mask #3). Acetone supersonic solution was used to remove positive photo-resist. Using S/D metal as a mask, the

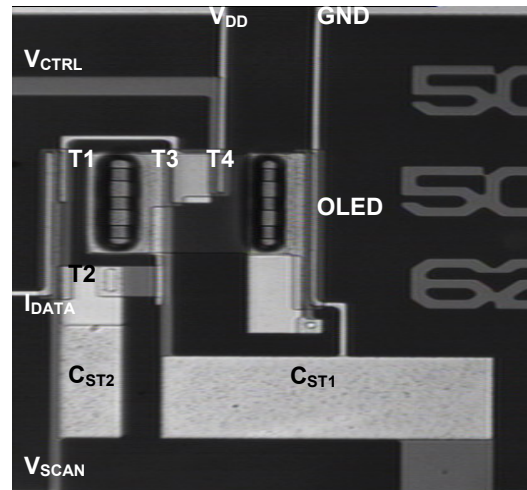
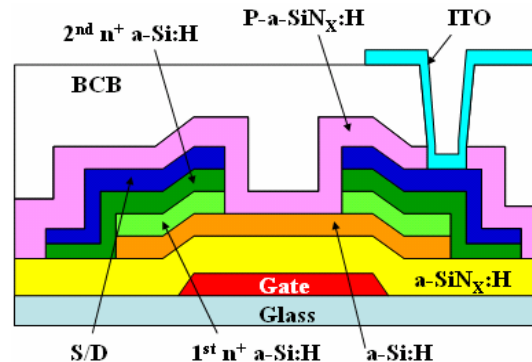


Figure 1 The schematic cross-section and top view of fabricated a-Si:H TFT pixel electrode circuit.

back-channel-etching was performed by reactive ion etching (RIE) to remove exposed n<sup>+</sup> a-Si:H layer between source and drain contacts. Finally, a-SiN<sub>x</sub>:H (3000Å) top passivation layer (P) was deposited by PECVD method followed by spin coating of the benzo-cyclo-butene (BCB) planarization layer that was cured in a furnace at 250°C in nitrogen ambient. Planarized a-Si:H TFTs by BCB were already reported previously [11, 12]. The pixel electrode indium tin oxide (ITO) was connected to S/D using via formed through the BCB / P-a-SiN<sub>x</sub>:H bi-layer by RIE (Mask #4). ITO (1200Å) was deposited by a DC magnetron sputtering at room temperature, and patterned by wet-etching (Mask #5) in a mixture of HCl, HNO<sub>3</sub>, and DI water at 60 °C [13]. Finally, ITO was thermally annealed at 250 °C in nitrogen.

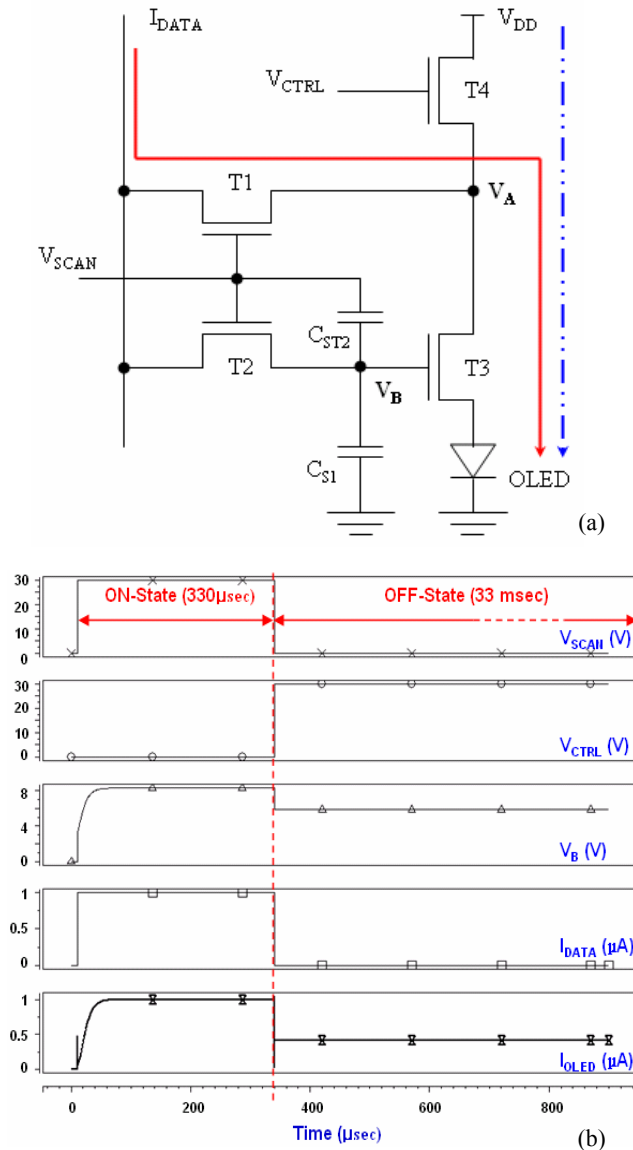


Figure 2 Schematic of (a) the cascaded-capacitor pixel electrode circuit and (b) operational wave forms simulated by HSPICE.

### 3. Operation and Measurement of Fabricated Current-Scaling Pixel Electrode Circuit

The fabricated current-driven pixel electrode circuit consists of three switching TFTs (T1, T2, and T4), one driving TFT (T3), and two storage capacitors ( $C_{ST1}$ ,  $C_{ST2}$ ) connected between a scan line and ground with a cascade structure, Figure 2 (a). Here we define  $I_{OLED\_ON}$  and  $I_{OLED\_OFF}$  as the current flowing through OLED during the ON- and OFF-state, respectively. During the ON-state,  $V_{SCAN}$  turns on the T1 and T2, and  $I_{DATA}$  ( $=I_{OLED\_ON}$ ) passes through T1 and T3 to OLED while the T4 remains turned-off by  $V_{CTRL}$ , shown as the solid line in Fig 2 (a). When the pixel changes from the ON- to OFF-state,  $V_{SCAN}$  turns off T1 and T2, and  $V_{CTRL}$  simultaneously turns on T4. Since gate bias of T3

( $V_{B\_ON}$ ) is reduced to  $V_{B\_OFF}$  by the ratio of cascaded capacitor ( $V_{B\_OFF} = V_{B\_ON} - \Delta V_{SCAN} \cdot C_{ST2} / (C_{ST1} + C_{ST2})$ ), a scaled-down data current ( $I_{OLED\_OFF}$ ) will flow through OLED, shown as the dashed line in Fig 2 (a). More details about this circuit operation can be found in [6].

To analyze the electrical performance of the pixel circuit, we measured  $I_{OLED\_ON}$  and  $I_{OLED\_OFF}$  flowing through the diode (OLED is represented here by a-Si:H TFT with gate and drain connected together) by applying  $I_{DATA}$ ,  $V_{CTRL}$ , and  $V_{SCAN}$  as shown in Fig. 2 (b). At the same time, constant DC  $V_{DD}$  and ground (GND) were applied. All measurements were done at room temperature, and all signals were applied using HP8110A function generator through a probe station. The time for ON- and OFF-state was set to 0.33 and 33ms, respectively. During ON-state,  $V_{SCAN}$  and  $V_{CTRL}$  were held at 30 and 0V, respectively while  $I_{DATA}$  was swept from 0.2 to 10  $\mu A$  for each measurement. During OFF-state,  $V_{SCAN}$  and  $V_{CTRL}$  were changed to 0 and 30V, respectively while  $I_{OLED}$  was measured with  $V_{DD}$  set at 30V. It should be noted that the  $I_{DATA}$  must be turned off when the circuit operation changes from ON- to OFF-state. Otherwise, the  $V_{DATA}$  measured when  $I_{DATA}$  is supplied will increase to high value ( $>40V$ ) to keep the current flowing when T1 and T2 are turned off, since the probe of  $I_{DATA}$  is set to the current supply mode. This high  $V_{DATA}$  can result in a large T2 leakage current, which increase the voltage at node B ( $V_{B\_OFF}$ ). Accordingly, the  $I_{OLED\_OFF}$  will also increase since  $V_{B\_OFF}$  increases.

Therefore, for proper circuit operation,  $I_{DATA}$  should be turned-off during OFF-state as shown in Fig. 2 (b). However, even though the  $I_{DATA}$  was turned off, the measured  $I_{OLED\_OFF}$  decreased slightly during OFF-state due to T2 current leakage, which originated from the voltage difference between source and drain. This current leakage causes the  $V_{B\_OFF}$  to decrease. To reduce the variation of  $V_{B\_OFF}$ , the following steps were taken: (i) the value of  $V_{DATA}$  during ON-state was measured while supplying DC  $I_{DATA}$ . Since the resistance of T1 was very small during ON-state, the voltage at node B ( $V_{B\_ON}$ ) was expected to be the same as measured  $V_{DATA}$ . (ii) Then,  $V_{DATA}$  obtained in step (i) was applied instead of  $I_{DATA}$  on the data line during ON-state. Since the  $V_{DATA}$  was same as  $V_{B\_ON}$  and it would supply the same current as  $I_{DATA}$ , the voltage levels during OFF-state between source and drain of T2 could be very similar so that the T2 leakage current was negligible and  $I_{OLED}$  was stable during OFF-state.

### 4. Electrical Properties of Current-Scaling Pixel Electrode Circuit

To investigate the current scaling ratio of the fabricated pixel electrode circuit, we changed the  $I_{DATA}$  from 0.2 to 10  $\mu A$  and measured the corresponding  $I_{OLED\_ON}$  and  $I_{OLED\_OFF}$  flowing through the diode for different ratios of cascaded-capacitors. In ON-state, the  $I_{OLED\_ON}$  is identical to the data current ( $I_{DATA}$ ) since the external driver directly controls the OLED current, Fig. 3 (a). When the pixel circuit operates in OFF-state, the diode current ( $I_{OLED\_OFF}$ ) is scaled-down by the ratio of cascade capacitor as discussed above and in [10]. From Fig. 3 (b), it is obvious that the larger  $C_{ST2}/C_{ST1}$  results in significant decrease of the  $I_{OLED\_OFF}$  at lower  $I_{DATA}$ . However, as shown previously [10], too large ratio of  $C_{ST2}/C_{ST1}$  ( $> 1/3$ ) resulted in the saturation of  $I_{OLED\_OFF}$ , which deteriorate the current scaling function eventually.

Since the OLED current value is different during ON- and OFF-state, we define the average OLED current ( $I_{AVE}$ ) during one

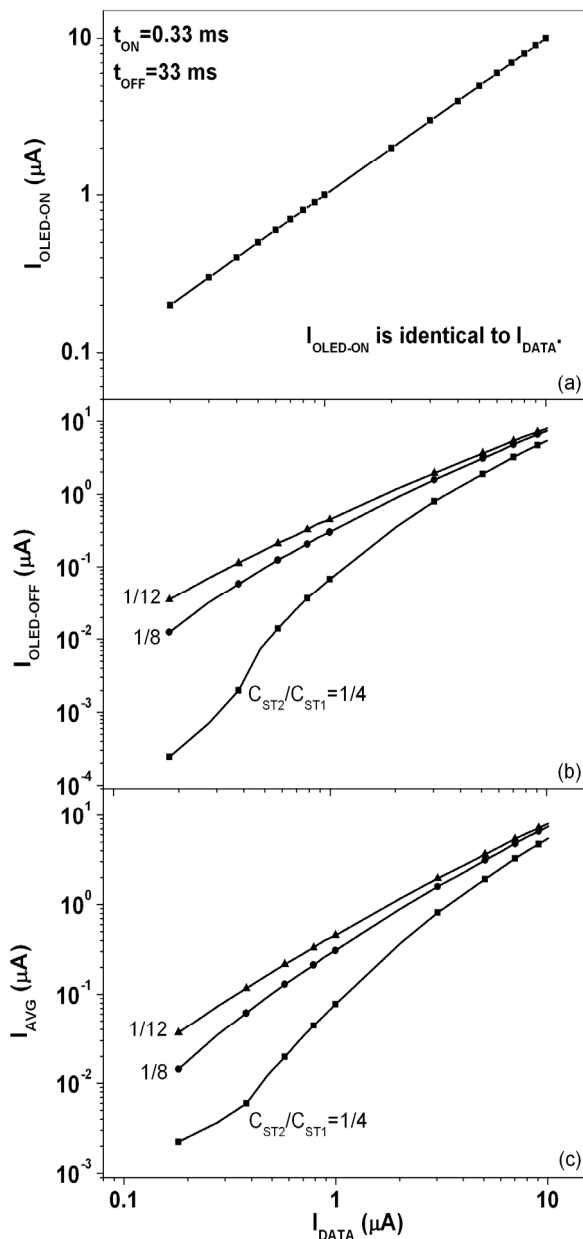


Figure 3 Variation of the measured  $I_{OLED\_ON}$ ,  $I_{OLED\_OFF}$  and  $I_{AVE}$  as a function of  $I_{DATA}$  ( $=I_{OLED\_ON}$ ) for various  $C_{ST2}/C_{ST1}$  ratios.

frame time [10] as  $I_{AVE} = (I_{OLED\_ON} \cdot t_{ON} + I_{OLED\_OFF} \cdot t_{OFF}) / (t_{ON} + t_{OFF})$ , where  $t_{ON}$  and  $t_{OFF}$  is the ON- and OFF- period during the frame time, respectively. The variation of  $I_{AVE}$  versus  $I_{DATA}$  in one frame period ( $t_{ON} + t_{OFF}$ ) for different  $C_{ST2}/C_{ST1}$  ratios is shown in Fig. 3 (c). Since the OFF-state period is much longer than ON-state, though  $I_{OLED\_OFF}$  is very small during OFF-state, it can reduce the  $I_{AVE}$  even if the  $I_{OLED\_ON}$  ( $=I_{DATA}$ ) is large. For example, the fabricated pixel electrode circuit can generate  $I_{AVE}$  ranging from 2 nA to 5  $\mu$ A while  $I_{DATA}$  swept from 0.2 to 10  $\mu$ A. Therefore, during one frame time, we can achieve very wide range

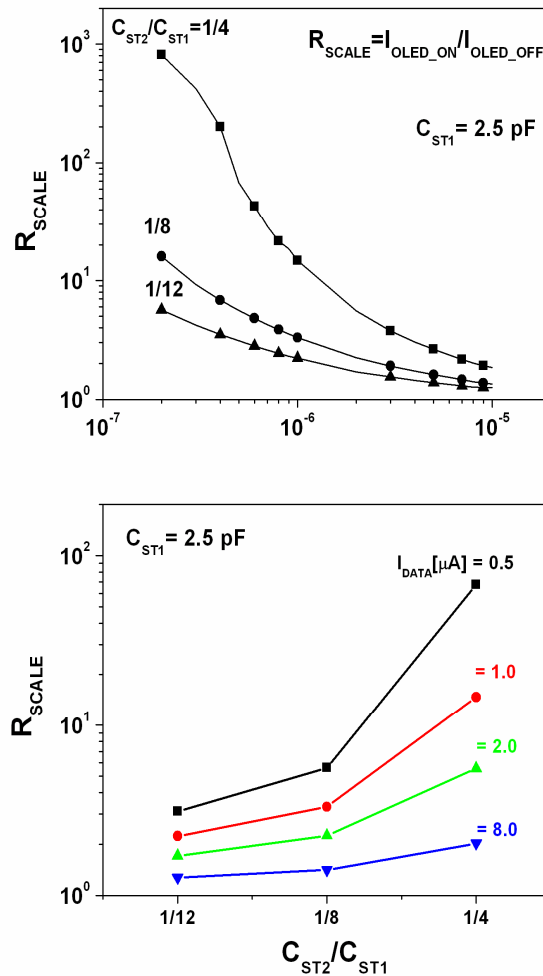


Figure 4 Variation of the measured current scaling ratio as a function of (a)  $I_{DATA}$  and (b) ratio of storage capacitances for fabricated cascaded-capacitor pixel circuit.

of OLED current levels by supplying high data current levels.

The evolution of the scaling ratio ( $R_{SCALE} = I_{OLED\_ON}/I_{OLED\_OFF}$ ) for different ratios of  $C_{ST2}/C_{ST1}$  as a function of  $I_{DATA}$  is shown in Fig. 4 (a). In this figure, we can see that for  $C_{ST2}/C_{ST1}=1/4$ ,  $R_{SCALE}$  decreases from 816 to 1.9 as  $I_{DATA}$  increases from 0.2 to 10  $\mu$ A, and an ideal non-linearity of  $R_{SCALE}$  can be achieved; e.g. a very high  $R_{SCALE}$  at low  $I_{DATA}$  levels (low gray scales) and a low  $R_{SCALE}$  at high  $I_{DATA}$  levels (high gray scales) can be produced. The variation of  $R_{SCALE}$  with the  $C_{ST2}/C_{ST1}$  is also shown in Fig. 4 (b). The measured results show that for fixed  $I_{DATA}$ ,  $R_{SCALE}$  increases as  $C_{ST2}$  increase from 210 to 625 fF, corresponding to an increase of  $C_{ST2}/C_{ST1}$  from 1/12 to 1/4. For constant  $C_{ST2}/C_{ST1}$ ,  $R_{SCALE}$  increases as  $I_{DATA}$  decreases as shown in Fig. 4 (a). Therefore, for a fixed ratio of  $C_{ST2}/C_{ST1}$  determined from the pixel electrode circuit design, we can expect the certain output OLED current range. These experimental results are comparable to simulated results previously reported [10].

## 5. Comparison with Other Pixel Electrode Circuits

To demonstrate the current-scaling function of the pixel electrode circuit in comparison with both the conventional current-driven [4] and current-mirror pixel circuits [7], we fabricated all three pixel electrode circuits using the same a-Si:H TFT technology, and measured  $I_{AVE}$  as a function of  $I_{DATA}$  for each pixel electrode circuit as shown in Fig. 5. Since  $I_{OLED\_ON}$  for all three circuits was identical to  $I_{DATA}$ , the current-driven circuit did not show any current-scaling function. On the contrary, while the current-mirror circuit showed only a fixed current-scaling by the ratio of  $T4/T3$  over all  $I_{DATA}$  range, the proposed cascaded-capacitor pixel circuit showed non-linear current-scaling function for variable current-scaling ratio depending on  $I_{DATA}$ . When  $I_{DATA}$  varies from  $2 \times 10^{-7}$  A to  $10^{-5}$  A, the proposed cascaded-capacitor pixel circuit with the ratio of  $C_{ST2}/C_{ST1}=1/4$  can provide  $I_{AVE}$  ranging from  $2 \times 10^{-9}$  A to  $5.4 \times 10^{-6}$  A. Hence much wider range  $I_{AVE}$  levels can be achieved by this circuit in comparison with the conventional current-driven pixel circuit ( $2 \times 10^{-7}$  to  $10^{-5}$  A) and the current-mirror pixel circuit ( $10^{-8}$  to  $2 \times 10^{-6}$  A).

## 6. Conclusion

When a low  $I_{DATA}$  is used to express a low gray scale, the conventional current-driven pixel circuit has a problem of slow programming time. On the contrary, when a high  $I_{DATA}$  is used to express a high gray scale, the current-mirror circuit has a problem of high power consumption due to a fixed current-scaling ratio. In the proposed circuit, by using cascaded-capacitors connected to the driving TFT, we could produce non-linear scaling-function that has a high scaling ratio at low current levels and a low scaling ratio at high current levels. Therefore, using this pixel circuit, we expect to avoid the unnecessary power consumption at high current levels and minimize the programming time at low current levels, which are supposed to be ideal characteristics for a high-resolution AM-OLED based on a-Si:H TFTs.

## 7. Acknowledgements

The author would like to thank Alex Kuo at the University of Michigan for useful discussions about a-Si:H TFT electrical and dynamic pixel electrode circuit measurements.

## 8. References

- [1] Y. He, R. Hattori, and J. Kanicki, "Improved a-Si:H TFT Pixel Electrode Circuits for Active-Matrix Organic Light Emitting Displays," *IEEE Trans. Electron Devices*, vol. **48**, pp. 1322-1325, 2001.
- [2] T. V. de Biggelaar, I. Camps, M. Childs, M. Fleuster, A. Giraldo, S. Godfrey, I. M. Hunter, M. T. Johnson, H. Lifka, R. Los, A. Sempel, J. M. Shannon, M. J. Trainor, R. W. Wilks, and N. D. Young, "Passive and Active Matrix Addressed Polymer Light Emitting Diode Displays," *Proceedings of SPIE*, vol. **4295**, pp. 134-146, 2001.
- [3] J. Kim, Y. Hong, and J. Kanicki, "Amorphous Silicon TFT-Based Active-Matrix Organic Polymer LEDs," *IEEE Electron Device Letters*, vol. **24**, pp. 451-453, 2003.
- [4] Y. Hong, J. Y. Nam, and J. Kanicki, "100 dpi 4-a-Si:H TFTs Active-Matrix Organic Polymer Light-Emitting Display,"

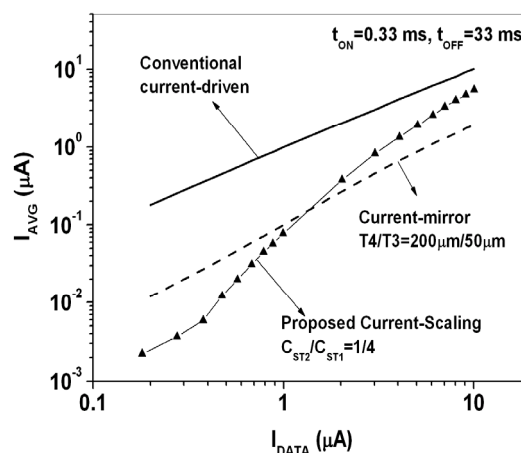


Figure 5 Comparison of  $I_{AVE}$  versus  $I_{DATA}$  for among conventional current-driven, current-mirror, and proposed pixel circuits.

IEEE J. Selected Topics in Quantum Electron., vol. **10**, pp. 16-25, 2004.

- [5] S. J. Ashtiani, P. Servati, D. Striakhilev, and A. Nathan, "A 3-TFT Current-Programmed Pixel Circuit for AMOLEDs," *IEEE Trans. Electron Devices*, vol. **52**, pp. 1514-1518, 2005.
- [6] Y. C. Lin, H. P. D. Shieh, and J. Kanicki, "A Novel Current-Scaling a-Si:H TFTs Pixel Electrode Circuit for AM-OLEDs," *IEEE Trans. Electron Devices*, vol. **52**, pp. 1123-1131, 2005.
- [7] A. Yumoto, M. Asano, H. Hasegawa, and M. Sekiya, "Pixel-Driving Methods for Large-Sized Poly-Si AM-OLED Displays," in *Proc. Int. Display Workshop*, pp. 1395-1398, 2001.
- [8] J. Lee, W. Nam, S. Jung, and M. Han, "A New Current Scaling Pixel Circuit for AMOLED," *IEEE Electron Device Lett.*, vol. **25**, pp. 280-282, 2004.
- [9] J. Lee, W. Nam, S. Han, and M. Han, "OLED Pixel Design Employing a Novel Current Scaling Scheme," *SID 03 Digest*, pp. 490-493, 2003.
- [10] Y. C. Lin, H. D. Shieh, C. C. Su, H. Lee, and J. Kanicki, "A Novel Current-Scaling a-Si:H TFTs Pixel Electrode Circuit for Active Matrix Organic Light-Emitting Displays," *SID 05 Digest*, pp. 846-848, 2005.
- [11] J. H. Lan and J. Kanicki, "Planarized Copper Gate Hydrogenated Amorphous-Silicon Thin-Film Transistors for AM-LCD's," *IEEE Electron Device Letters*, vol. **20**, pp. 129-131, 1999.
- [12] J. H. Lan and J. Kanicki, "Planarization Technology of a-Si:H TFTs for AM-LCDs," *Proceedings of SPIE*, vol. **3421**, pp. 170-182, 1988.
- [13] J. H. Lan, J. Kanicki, A. Catalano, J. Keane, W. den Boer, and T. Fu, "Patterning of Transparent Conducting Oxide Thin Films by Wet Etching for a-Si:H TFT LCDs," *J. Electronic Materials*, vol. **25**, pp. 1806-1817, 1996.